

~~SECRET~~

UNCLASSIFIED
RM L51H31

DEC 17 1951

NACA RM L51H31



RESEARCH MEMORANDUM

PRELIMINARY INVESTIGATION OF THE TRANSFER OF HEAT FROM
A FLAT PLATE AT A MACH NUMBER OF 1.5

By M. A. Emmons, Jr., and R. F. Blanchard

Langley Aeronautical Laboratory
Langley Field, Va.

CLASSIFICATION CANCELLED

Authority J. W. Crowley Date 12/11/53
EO 12501
By 202A 1/11/54 See rule
R71821

CLASSIFIED DOCUMENT

This material contains information affecting the National Defense of the United States within the meaning of the espionage laws, Title 18, U.S.C., Secs. 793 and 794, the transmission or revelation of which in any manner to unauthorized person is prohibited by law.

NATIONAL ADVISORY COMMITTEE FOR AERONAUTICS

WASHINGTON
December 13, 1951

UNCLASSIFIED

~~SECRET~~

NACA LIBRARY
LANGLEY AERONAUTICAL LABORATORY
Langley Field, Va.



UNCLASSIFIED

NATIONAL ADVISORY COMMITTEE FOR AERONAUTICS

RESEARCH MEMORANDUM

PRELIMINARY INVESTIGATION OF THE TRANSFER OF HEAT FROM

A FLAT PLATE AT A MACH NUMBER OF 1.5

By M. A. Emmons, Jr., and R. F. Blanchard

SUMMARY

Surface temperatures and heat transfer to the air stream have been measured for turbulent flow over a flat plate at a Mach number of 1.5 and at a Reynolds number, based on the momentum thickness of the boundary layer, of approximately 5000. Preliminary data are presented and the surface heat-transfer coefficients calculated from these data are considered to be accurate to ± 2.6 percent at a temperature potential of 50° F. These data are in good agreement with the results produced by applying modifications obtained from published information to existing subsonic theories.

INTRODUCTION

Aerodynamic heating of external surfaces constitutes a major problem in the design of supersonic aircraft and experimental heat-transfer data at supersonic speeds are in great demand. Heat-transfer coefficients for subsonic flow in tubes have been thoroughly investigated and satisfactory agreement for engineering purposes exists among data from many sources. There has been far less experimental work done for subsonic flow over flat plates and much reliance has been placed on heat-transfer coefficients obtained from friction coefficients through use of the Reynolds analogy. Experimental heat-transfer data at supersonic speeds are fragmentary, results having been obtained for flow in tubes, reference 1, and over cones, references 2 and 3. Reference 4 presents qualitative measurements of the heat transfer and skin friction for supersonic flow over a flat plate and makes use of the Von Kármán extension of the Reynolds analogy at supersonic speeds. The present investigation was undertaken because of the lack of experimental data on flat plates at supersonic speeds.

The present paper deals with preliminary heat-transfer measurements on a flat plate at a Mach number of 1.5 made by a technique especially

UNCLASSIFIED

suited for correlating local heat-transfer coefficients with local boundary-layer parameters.

SYMBOLS

A	heat-transfer area, square feet
c_f	local skin-friction coefficient
c_p	specific heat at constant pressure, Btu/lb °F
C	conversion factor from electrical to heat units
g	gravitational constant, feet per second ²
h_e	heat-transfer coefficient, based on difference between elevated and adiabatic wall temperature, Btu/sec ft ² °F
I	current input to measuring surface, amperes
I_t	total current to bridge, amperes
K	constant, determined by fixed resistors of bridge
M	free-stream Mach number
P	power input to surface, watts
Pr	Prandtl number
Q	heat transfer to air stream, Btu/sec
R_b	balancing resistance, ohms
R	surface resistance, ohms
Re_θ	Reynolds number based on momentum thickness of the boundary layer
S_t	Stanton number ($h_e/c_p g \theta$)
T_0	stream stagnation temperature, degrees Fahrenheit
t	mean stream temperature, degrees Fahrenheit
T_{ad}	adiabatic wall temperature, degrees Fahrenheit

T	heated surface temperature, degrees Fahrenheit
ΔT	temperature potential, degrees Fahrenheit ($T - T_{ad}$)
u	velocity in boundary layer, feet per second
U	free-stream velocity, feet per second
δ	boundary-layer thickness, inches
δ^*	boundary-layer displacement thickness, inches
θ	boundary-layer momentum thickness
$H = \frac{\delta^*}{\theta}$	
ρ	density, slugs per cubic foot
μ	absolute viscosity, slugs per foot-second
τ_0	shear stress at the wall, pounds per square foot

APPARATUS AND METHOD

Test Installation

The test model chosen was a flat steel plate 4 inches wide, 18 inches long, 3/4 inch thick, with the lower surface beveled to form an 8° leading edge. The heat-transfer instrument was located 4 inches from the leading edge of the test plate. The test model is presented in figure 1 and a close-up of the heat-transfer instrument imbedded in the mounting plate is presented in figure 2. Extreme care was exercised in setting the mounting frame exactly flush with the test surface.

The flat plate was installed in the test section of an 8.8 inches high by 4 inches wide, two-dimensional supersonic tunnel. The test surface containing the instrument made a rectangular channel 2 inches high by 4 inches wide with the top surface of the tunnel. The tunnel was operated at its design Mach number of 1.5, a total pressure of 2 atmospheres, and at a stagnation temperature of 220° F.

Four total-pressure tubes located directly downstream of the heat-transfer-measuring instrument, in conjunction with static-pressure orifices on either side of the instrument were used to determine the boundary-layer velocity profile.

Instrument

The instrument consists of three elements, front or measuring surface, and back and peripheral guard surfaces, figure 3. The guard surfaces are maintained at the same temperature as the measuring surface to prevent heat loss from the measuring surface. Each surface is electrically insulated and forms the unknown in an independent Wheatstone bridge circuit. Resistance changes of the three surfaces are calibrated in terms of temperature.

Physically, the instrument forms a 1-inch-square glass unit 1/8-inch thick, composed of two first-surfaced rhodium coated mirrors arranged back to back and separated by a 0.005-inch air gap, with resistance wire cemented around the periphery of the complete unit. The measuring and back guard surfaces are rhodium coatings approximately 20 microinches thick. Three grooves 0.75-inch long, 0.01-inch wide by 0.0005-inch deep are cut through each rhodium surface to increase the effective length of electrical path, figure 3.

Preliminary resistance measurements of the various rhodium surfaces used indicated a range of 75 to 125 ohms, with the average being 100 ohms. The peripheral guard winding was formed from 0.002-inch-diameter nickel wire having a total resistance of 75 ohms.

Surface resistance, and therefore temperature, is determined by obtaining a null point balance on the bridge. The bridge circuits are set up to give an approximate ratio of 10:1 and so arranged that the individual surfaces can be heated electrically and their resistances measured simultaneously. Measurement of surface resistance while electrical heat is being supplied is accomplished by proper selection of the bridge components. Power ratings of the other arms of the bridge are chosen to prevent resistance changes due to overheating at high bridge currents. A schematic wiring diagram of a typical bridge circuit with nominal values of the bridge components is shown in figure 4. By using values of total current input and balancing resistance with conventional bridge relationships, the power input to each surface is expressed as:

$$P = I^2 R = KR_b I_t^2 \quad (1)$$

All power supplied to the measuring surface is transferred to the air stream provided no heat is lost to the surrounding body. This loss is prevented by maintaining the back and peripheral guard surfaces at the same temperature as the measuring surface.

Heat dissipation to the air stream is expressed as:

$$Q = CP \quad (2)$$

It has been shown (reference 5) that the temperature potential (temperature difference) to use in computing heat-transfer coefficients should be the difference between the surface temperature with heat transfer and the surface temperature in the absence of heat transfer. The temperature in the absence of heat transfer is defined as the adiabatic surface temperature.

Temperatures with heat transfer are measured while supplying power to the surface. Measurements of adiabatic surface temperatures are obtained with the bridge current limited to a value for which surface heating is negligible. The surface heat-transfer coefficient is obtained from the relationship:

$$h_e = \frac{Q}{A\Delta T} \quad (3)$$

Calibration.- The calibration was accomplished by suspending the instrument in an agitated liquid bath. Bath temperatures were obtained to an accuracy of $\pm 0.25^\circ$ F with a certified mercury-in-glass thermometer. Readings of individual surface resistances and the corresponding bath temperature were taken at several uniformly distributed calibration points throughout the temperature range of 75° F to 300° F. Readings were recorded after the rate of change of bath temperature was less than 0.1° F per minute. Prior to putting an instrument into service not less than two complete calibrations were made to insure stability. In addition, room temperature checks for drift were made before and after every run. Experience has shown that at no time did the slope of the calibration change, any deviation appearing as a shift of the entire curve. A typical calibration of balancing arm resistance against temperature is shown in figure 5.

Accuracy.- The over-all accuracy of the instrument was obtained by a combination of estimation and measurement and depended on the magnitudes of many component errors. The accuracy analysis for this instrument has been made on the following basis: Fixed errors were evaluated from laboratory standards and reasonable values assigned to all other uncertainties. The resultant accuracy of the heat-transfer coefficient has been calculated for two conditions. First, the individual errors were combined in a manner to make the resultant error a maximum. This has been termed the "maximum possible" error and will not be exceeded for all components operating under normal laboratory conditions and with no malfunctioning of parts, instruments, or operator. Second, all the indeterminate errors were assumed to be in the same direction and all

reading errors nonexistent. This condition represents an expected precision and for careful operating practices is close to the actual accuracy of the instrument.

The resultant accuracy is also a function of temperature potential; therefore the two error conditions have been calculated for three representative temperature potentials.

The resultant accuracy of the heat-transfer coefficient for the two error conditions and three temperature potentials is presented below:

ΔT (°F)	"Maximum possible" error (percent)	Expected precision (percent)
50	±5.0	±2.6
25	±7.2	±2.8
15	±10.0	±3.0

As the instrument heat-transfer surface possesses finite area, the measured temperatures represent average values.

Main-stream stagnation temperatures were obtained with a thermocouple mounted in a stagnation cup and read with a self-balancing potentiometer to an accuracy of $\pm 1.0^\circ$ F.

Test Procedure

Heat-transfer and temperature-measuring procedures will be given in detail for the front surface. In operation, the back and peripheral guard surfaces follow the same pattern.

For measuring adiabatic temperatures, the bridge current was limited to 10 milliamperes; this small current produced negligible surface heating but permitted the instrument to function as a resistance thermometer. Temperatures above adiabatic were obtained by adjusting the balancing resistance to correspond with the desired temperature and manually increasing the current input until the bridge was again balanced. Bringing the three surfaces to balance at the same time required a technique which was developed with operation of the instrument. When all three surfaces were balanced, the readings of current input to the bridge, the value of balancing resistance, and the use of equation (1) allowed the heat input to the measuring surface to be calculated. The two guard surfaces were maintained at the same

temperature as the measuring surface; therefore, all heat input to the measuring surface was transferred to the air stream. Between each pair of elevated-temperature conditions, readings of adiabatic temperature were taken. The correct adiabatic surface temperature was obtained by recording all readings against time. This procedure eliminated the effect of the slow drift of tunnel temperature, 1° F per hour, and the associated drift of adiabatic surface temperature. Use of equations (2) and (3) permitted calculation of the surface heat-transfer coefficient. The guard surfaces were maintained at the measuring surface temperature; therefore, only the heat input to the measuring surface was used in the calculation.

It was realized that radiation of heat energy from measuring surface to tunnel walls introduced an error in the data. The magnitude of this effect was calculated for the worst temperature condition encountered, and found to be less than 0.1 percent of the total heat transferred. The correction for radiation was, therefore, neglected.

For each heat-transfer condition pressure data were obtained; boundary-layer velocity profiles and local Mach numbers were then calculated from these data.

RESULTS AND DISCUSSION

Flow Conditions

The test plate was aligned with the air stream to give a constant Mach number over the test surface. Schlieren observation showed a Mach line, originating at the plate leading edge and reflecting from the tunnel wall, striking the test surface in the vicinity of the instrument. No deflection of the line was observed, however, and constancy of the static pressure in the region occupied by the measuring surface together with this absence of deflection indicated that the disturbance seen was of negligible strength. The static-pressure distribution on the test surface indicated a Mach number range of 1.47 to 1.50, the local Mach number at the heat-transfer measuring station being 1.48. The total pressure obtained in a low-velocity region upstream of the tunnel is used in obtaining these Mach numbers.

Boundary-layer data were obtained for each temperature condition. A typical boundary-layer velocity profile is presented in figure 6. This profile indicates a turbulent boundary layer approximately 0.1 inch thick and closely follows an exponential power law of $1/6.3$; no change in these values was detected at any value of heat input. For purposes of comparison, the boundary-layer-thickness parameters and shape factor have been computed by using relations for incompressible flow and are shown in figure 6.

Heat Transfer

Rate of heat transfer.- Essential to the definition of a heat-transfer coefficient is the definition of the temperature potential on which it is based. In reference 5, it was found that a coefficient based on the elevation of surface temperature above adiabatic wall temperature was substantially independent of the rate of heat transfer and temperature potential. This independence of rate of heat transfer and temperature potential is confirmed in the current experiments.

The heat transmitted from the measuring surface to the air stream is plotted in figure 7 as a function of temperature differences. The temperature for the solid line is the difference between elevated surface temperature and temperature of the identical surface in the unheated condition. The temperature potential for the dashed-line curve is the difference between elevated surface temperature and stagnation temperature of the main air stream. Both curves are quite linear and that based on the adiabatic surface temperature passes through the origin of the coordinates. Inasmuch as the heat-transfer coefficient is the ratio of ordinate to abscissa of figure 7, it is apparent that the solid line, based upon adiabatic wall temperature, will yield a constant coefficient. At any single value of heat input, the difference between the two curves represents the difference between stream stagnation and adiabatic wall temperature. As there was some change in stagnation temperature during the time of heat-transfer measurements, there is a slight deviation from parallelism of the two curves, this variation is, however, almost too small to be detectable.

Recovery factor.- It is of interest to compare the depression of adiabatic wall temperature below stagnation with that which would have been predicted from the analysis of reference 6. This depression is expressed as:

$$(T_0 - t)(1 - Pr^m) \quad (4)$$

where m equals $1/2$ for a laminar boundary layer and $1/3$ for a turbulent boundary layer (reference 6). The temperature depression calculated from this relation for the conditions of figure 7 and at a Prandtl number of 0.69 is 35.1° F for a laminar boundary layer and 24.1° F for a turbulent boundary layer. The value of 26.8° F shown in figure 7 is within 2.7° F of that computed from reference 6 for a turbulent boundary layer.

Stanton number.- Values of the Stanton number for an average value of heat-transfer coefficient of 0.023 (obtained from the solid curve of fig. 7), and based on the difference between heated-plate temperature

and adiabatic wall temperature are presented in figure 8. These data are plotted against temperature potential, that is, the difference between heated-plate and adiabatic wall temperature. The solid curve is obtained by evaluating the thermodynamic properties of the air at the adiabatic wall temperature, and the dashed curve by evaluating the air properties at the free-stream static temperature. It is evident from the two curves of figure 8 that for the identification of a Stanton number at high Mach number it is necessary to stipulate the temperature base for evaluating the thermodynamic properties of the air.

Estimated values for comparison with the experimental values.-

Comparison of the results of this investigation with existing theories will be made with the use of the Von Kármán extension of the Reynolds analogy (reference 7) and the Squire and Young skin-friction relation of reference 8. The Von Kármán extension of the Reynolds analogy, reference 7, was originally derived for low-speed flows in pipes by using mean values of velocity and temperature. This relation is expressed in the symbols of this paper as

$$\frac{1}{St} = \frac{2}{c_f} + 5 \sqrt{\frac{2}{c_f}} \left\{ (Pr - 1) + \log_e \left[1 + 0.83(Pr - 1) \right] \right\} \quad (5)$$

where $c_f = \frac{\tau_0}{\frac{1}{2}\rho U^2}$.

The Squire and Young skin-friction relation of reference 8 relates the local skin-friction coefficient to a Reynolds number based on the momentum thickness of the boundary layer, the free-stream velocity, and stream properties evaluated at free-stream temperature. This relation is expressed as

$$c_f = \frac{2}{\left[2.557 \log_e (4.075 Re_\theta) \right]^2} \quad (6)$$

Equations (5) and (6) permit the calculation of the local skin-friction coefficient and Stanton number from a Reynolds number based on the momentum thickness of the boundary layer for incompressible flow. At high speeds, however, because of compressibility effects, there is a considerable variation across the boundary layer of the physical

properties of the air and a departure of the skin-friction coefficient and Stanton number from incompressible values is to be anticipated. Two proposals, from published sources, for modifying the incompressible relation of skin friction to Reynolds number for use at supersonic Mach numbers have been adapted to the particular skin-friction - Reynolds number relationship of this paper and are presented in the following sections.

Method of reference 9.- The allowance for compressibility effects as proposed by Monaghan (reference 9) is substantially as follows. The distance-based Reynolds number is determined by evaluating the air properties at the adiabatic wall temperature. An "incompressible Reynolds number" is obtained from this value by multiplying by the ratio of free-stream temperature to adiabatic wall temperature. The true friction coefficient is then considered to be that corresponding in incompressible relationships to this "incompressible Reynolds number;" the air density used in determining the wall friction from the friction coefficient is based upon wall temperature. For comparison with the present experiments the assumption has been made that the general procedure of reference 9 is also applicable where the Reynolds number is based upon boundary-layer thicknesses instead of upon distances. In order to obtain a Stanton number from the friction coefficient so obtained, the additional assumption is made, following the precedent of reference 4, that equation (5) is sufficiently accurate. Like the friction coefficient, the physical properties of air appearing in the Stanton number are evaluated in terms of the wall temperature.

The procedure of reference 9 as adapted to the present investigation is illustrated in figure 9. The curve on the right in figure 9 represents the Squire and Young relationship, equation (6), of friction coefficient c_f to Reynolds number Re_θ for incompressible flow. The curve on the left is the curve of equation (5), evaluated for a Prandtl number corresponding to the adiabatic wall temperature. The latter curve is not materially displaced if the Prandtl number is evaluated at free-stream static temperature. The point in figure 9 marked ① is the Reynolds number of the test data evaluated at wall temperature. The point marked ② is the corresponding "incompressible Reynolds number." The dotted line indicates evaluation of the friction coefficient and the Stanton number. The experimental Stanton number which is identified by ③ is about 4 percent less than the value calculated by the adapted procedure of reference 9.

Method of reference 10.- The authors of reference 10 propose an expression for the influence of compressibility effects on the friction coefficient in the form of a function of Mach number. This factor is applied as a multiplier to the incompressible relationship of friction

factor to distance-based Reynolds number evaluated at stream static temperature and is expressed as

$$F_M = \frac{1}{\left(1 + \frac{M^2}{5}\right)^{0.467}} \quad (7)$$

As in the case previously discussed, the adaption to the present investigation involves the assumption of applicability of the procedure to Reynolds numbers based upon boundary-layer thicknesses and also the applicability of equation (5). When using the procedure of reference 10, however, the friction coefficients and Stanton numbers are based upon free-stream static temperature instead of wall temperature as was the case with the analysis of reference 9. Figure 10 illustrates the procedure of reference 10 as adapted to the present investigation. The curve on the right in figure 10 is for the friction-coefficient - Reynolds number relationship, equation (6), evaluated at stream static temperature, and modified by the Mach number term of reference 10 for a stream Mach number of 1.48:

$$c_f = \frac{2}{\left[2.557 \log_e(4.075 Re_\theta)\right]^2} \frac{1}{\left(1 + \frac{M^2}{5}\right)^{0.467}} \quad (8)$$

The curve on the left in figure 10 (identical with the left-hand curve of fig. 9) gives the relation of Stanton number to friction coefficient. The dotted line, starting with the experimental boundary-layer Reynolds number leads to the estimated supersonic friction coefficient and Stanton number, both based on free-stream static temperature. The corresponding experimental value is identified as the solid triangular symbol on the abscissa of figure 10 and agrees with the calculated value within the readability of the curve.

CONCLUDING REMARKS

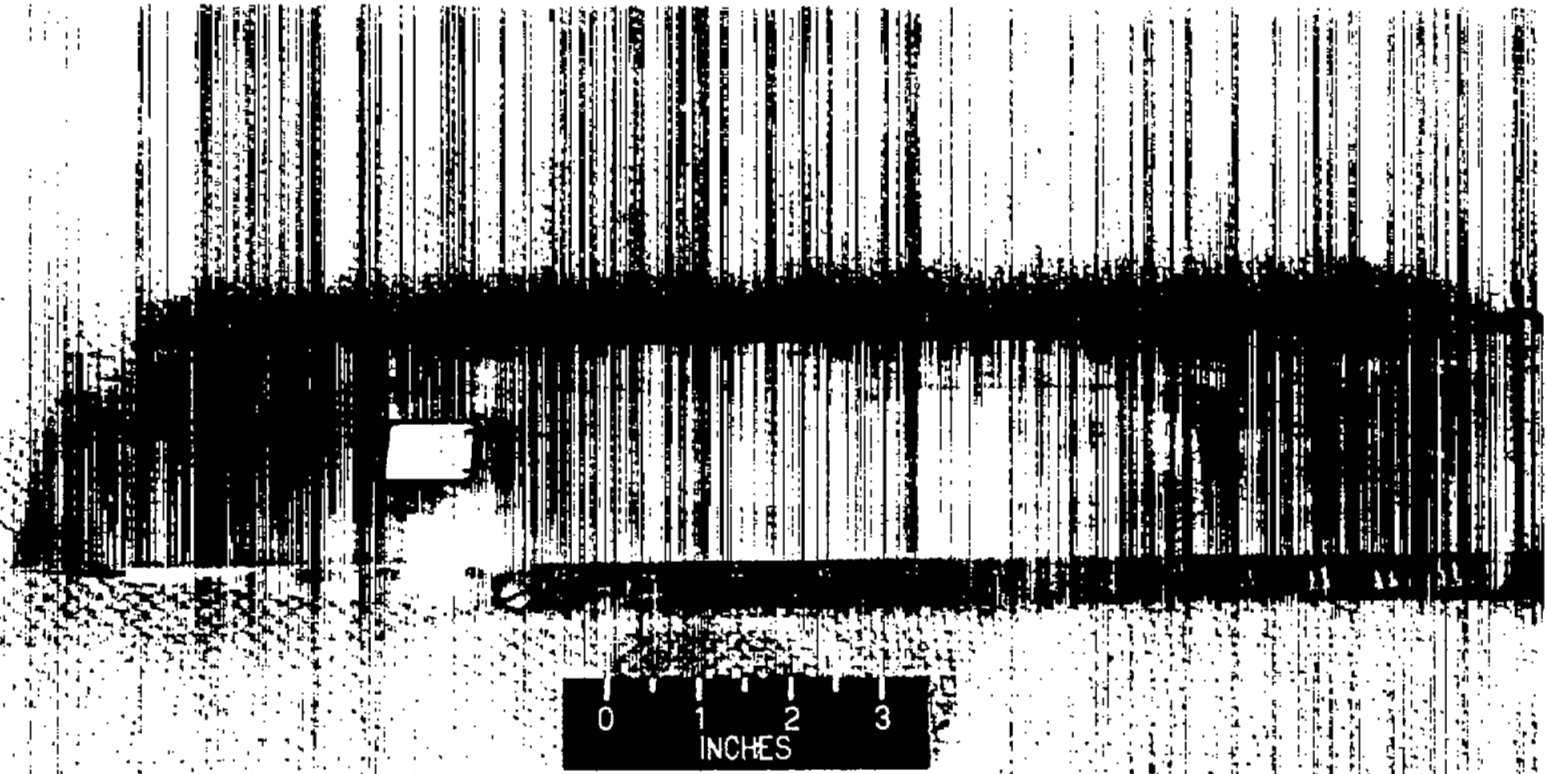
The data obtained to date, not covering a range of Reynolds and Mach numbers, are insufficient to justify any generalizations as to heat-transfer coefficients in supersonic flow. The accuracy of the measurements, however, as indicated by the close agreement between coefficients obtained at several different rates of heat transfer, is

such as to warrant considerable confidence in the results so far obtained. Two methods of extending subsonic theories to supersonic speeds, while similar in principle but differing in procedure, have been compared with the experimental values obtained and good agreement realized.

Langley Aeronautical Laboratory
National Advisory Committee for Aeronautics
Langley Field, Va.

REFERENCES

1. Kaye, Joseph, Keenan, Joseph H., and McAdams, William H.: Measurements of Friction Coefficients, Recovery Factors, and Heat-Transfer Coefficients for Supersonic Flow of Air in a Pipe. M.I.T. Tech. Rep. No. 6418-1, June 1, 1949.
2. Scherrer, Richard, Wimbrow, William R., and Gowen, Forrest E.: Heat-Transfer and Boundary-Layer Transition on a Heated 20° Cone at a Mach Number of 1.53. NACA RM A8L28, 1949.
3. Scherrer, Richard, and Gowen, Forrest E.: Comparison of Theoretical and Experimental Heat Transfer on a Cooled 20° Cone with a Laminar Boundary Layer at a Mach Number of 2.02. NACA TN 2087, 1950.
4. Johnson, J. E., and Monaghan, R. J.: Measurement of Heat Transfer and Skin Friction at Supersonic Speeds: Preliminary Results of Measurements on Flat Plate at Mach Number of 2.5. TN No. Aero. 1994, S.D. 91, British R.A.E., April 1949.
5. McAdams, William H., Nicolai, Lloyd A., and Keenan, Joseph H.: Measurements of Recovery Factors and Coefficients of Heat Transfer in a Tube for Subsonic Flow of Air. NACA TN 985, 1945.
6. Squire, H. B.: Heat Transfer Calculation for Aerofoils. R. & M. No. 1986, British A.R.C., 1946.
7. Fluid Motion Panel of the Aeronautical Research Committee and Others: Modern Developments in Fluid Dynamics. Vols. I and II, S. Goldstein, ed., Clarendon Press (Oxford), 1938.
8. Squire, H. B., and Young, A. D.: The Calculations of the Profile Drag of Aerofoils. R. & M. No. 1838, British A.R.C., 1938.
9. Monaghan, R. J.: Comparison between Experimental Measurements and a Suggested Formula for the Variation of Turbulent Skin-Friction in Compressible Flow. TN No. Aero. 2037, British R.A.E., Feb. 1950.
10. Rubesin, Morris W., Maydew, Randall C., and Varga, Steven A.: An Analytical and Experimental Investigation of the Skin Friction of the Turbulent Boundary Layer on a Flat Plate at Supersonic Speeds. NACA TN 2305, 1951.



NACA
I-3374

Figure 1.- Test model with heat-transfer instrument installed.

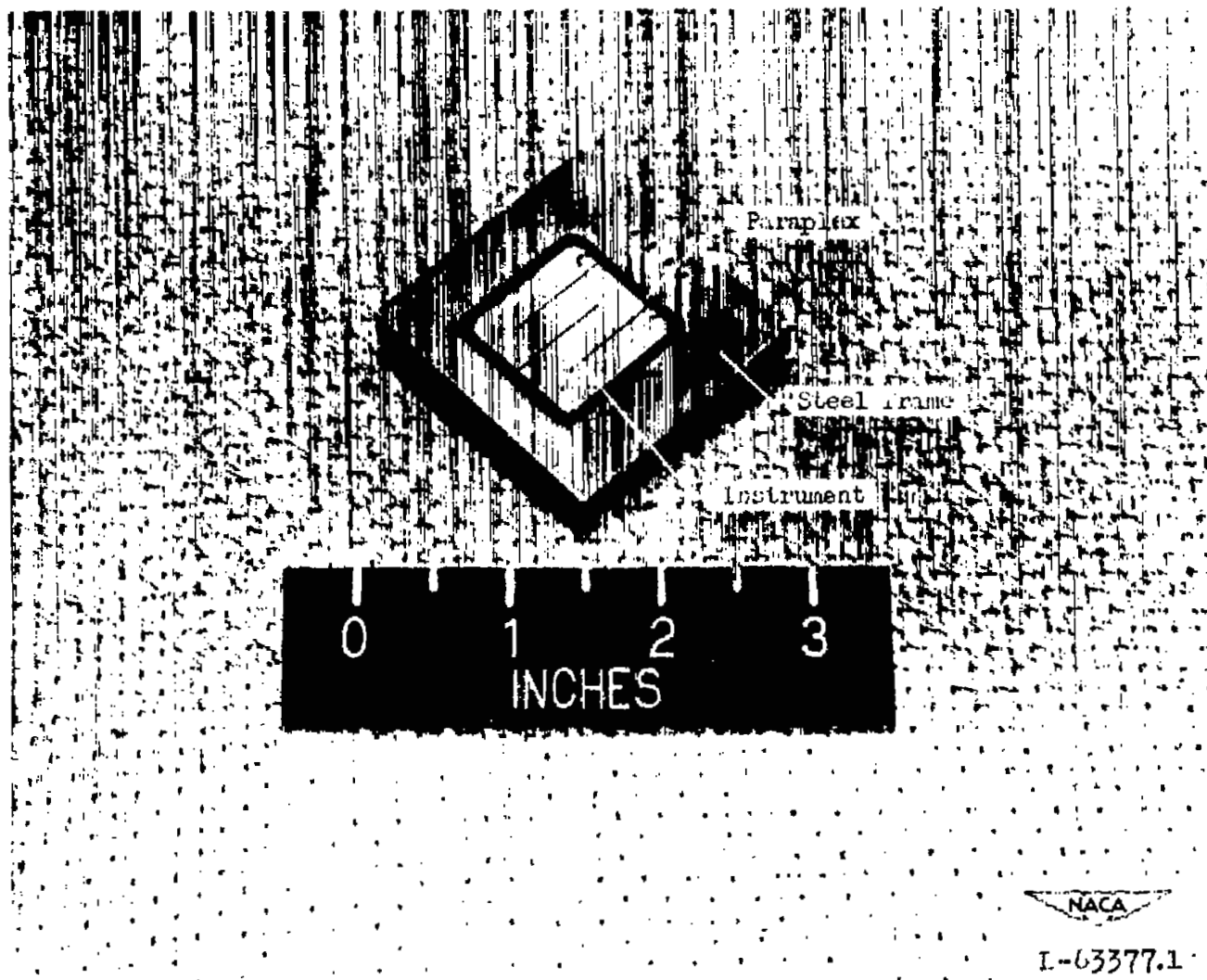


Figure 2.- Heat-transfer instrument imbedded in steel mounting frame.

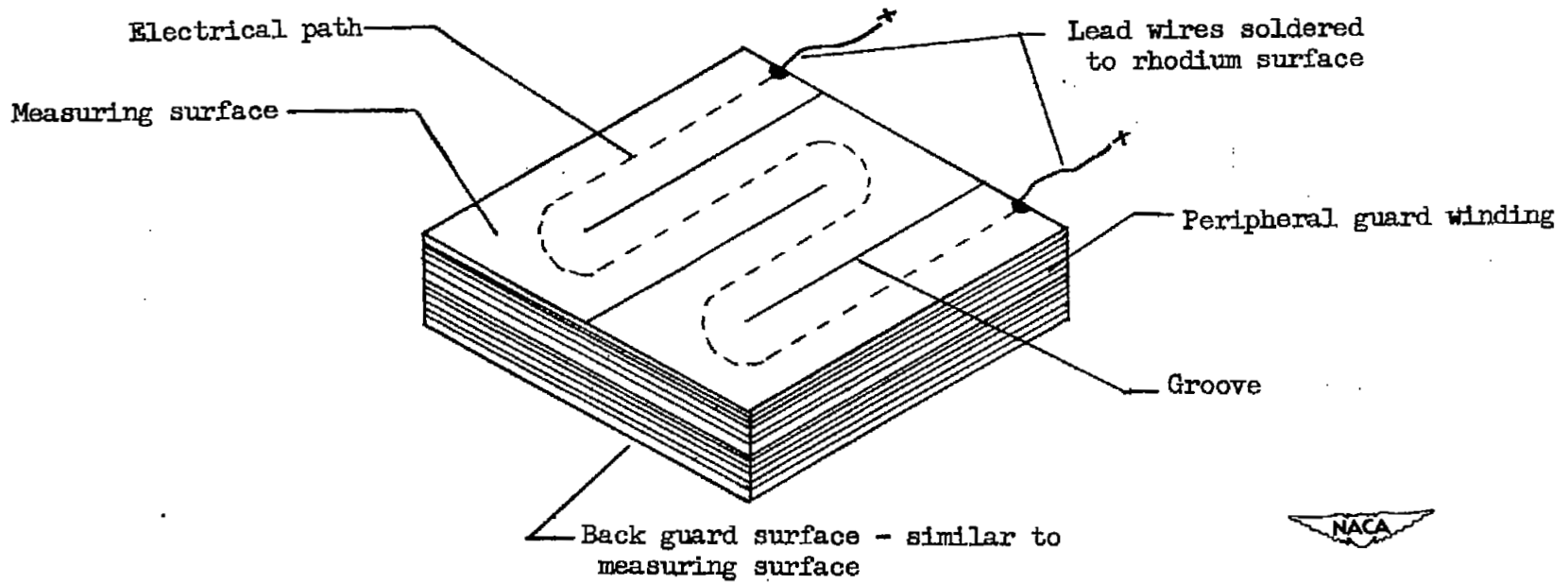


Figure 3.- Heat-transfer instrument assembly.

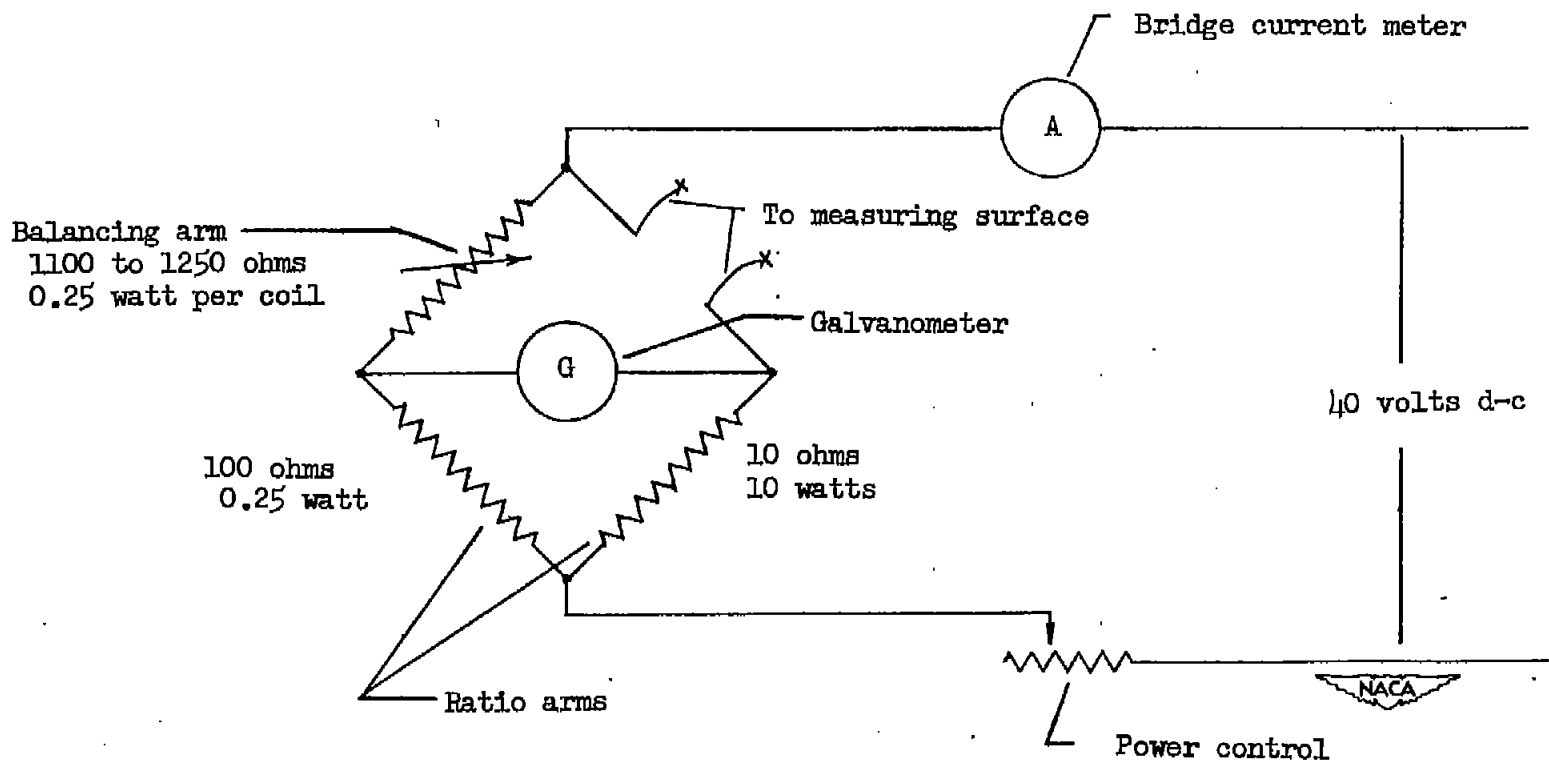


Figure 4.- Wiring diagram of typical control bridge.

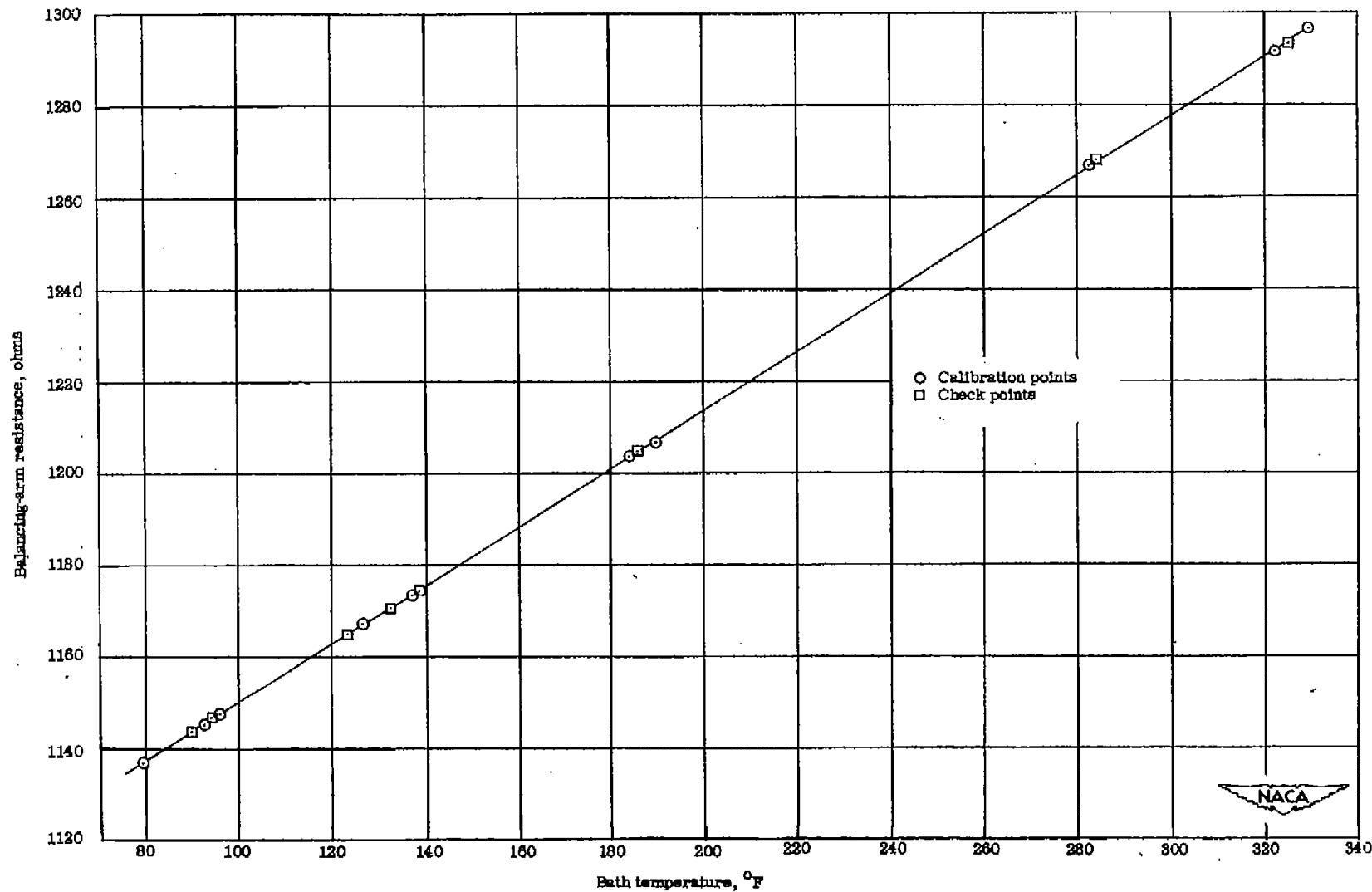


Figure 5.- Typical calibration curve for one surface of heat-transfer instrument.

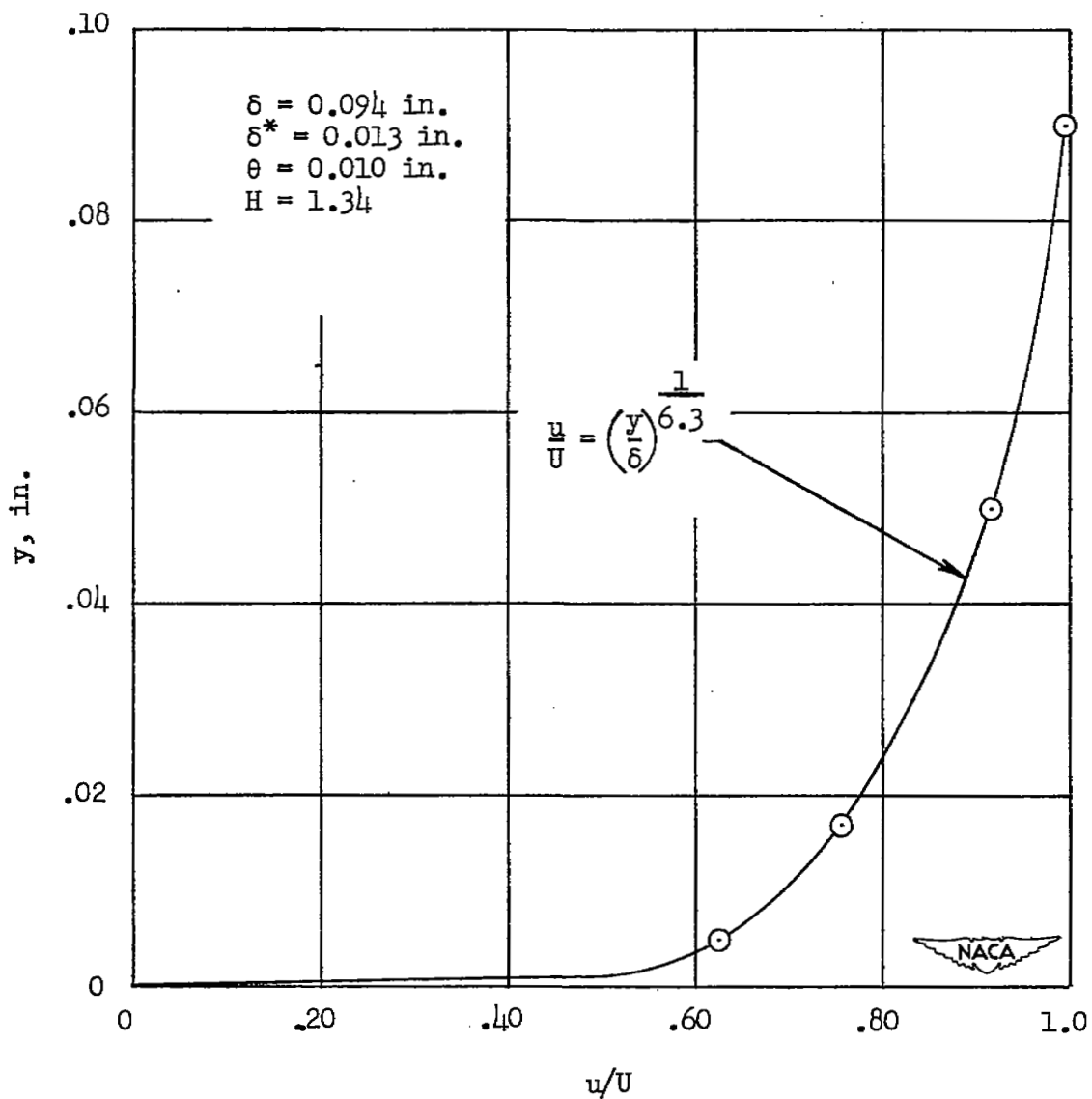


Figure 6.- Boundary-layer velocity profile at heat-transfer station.

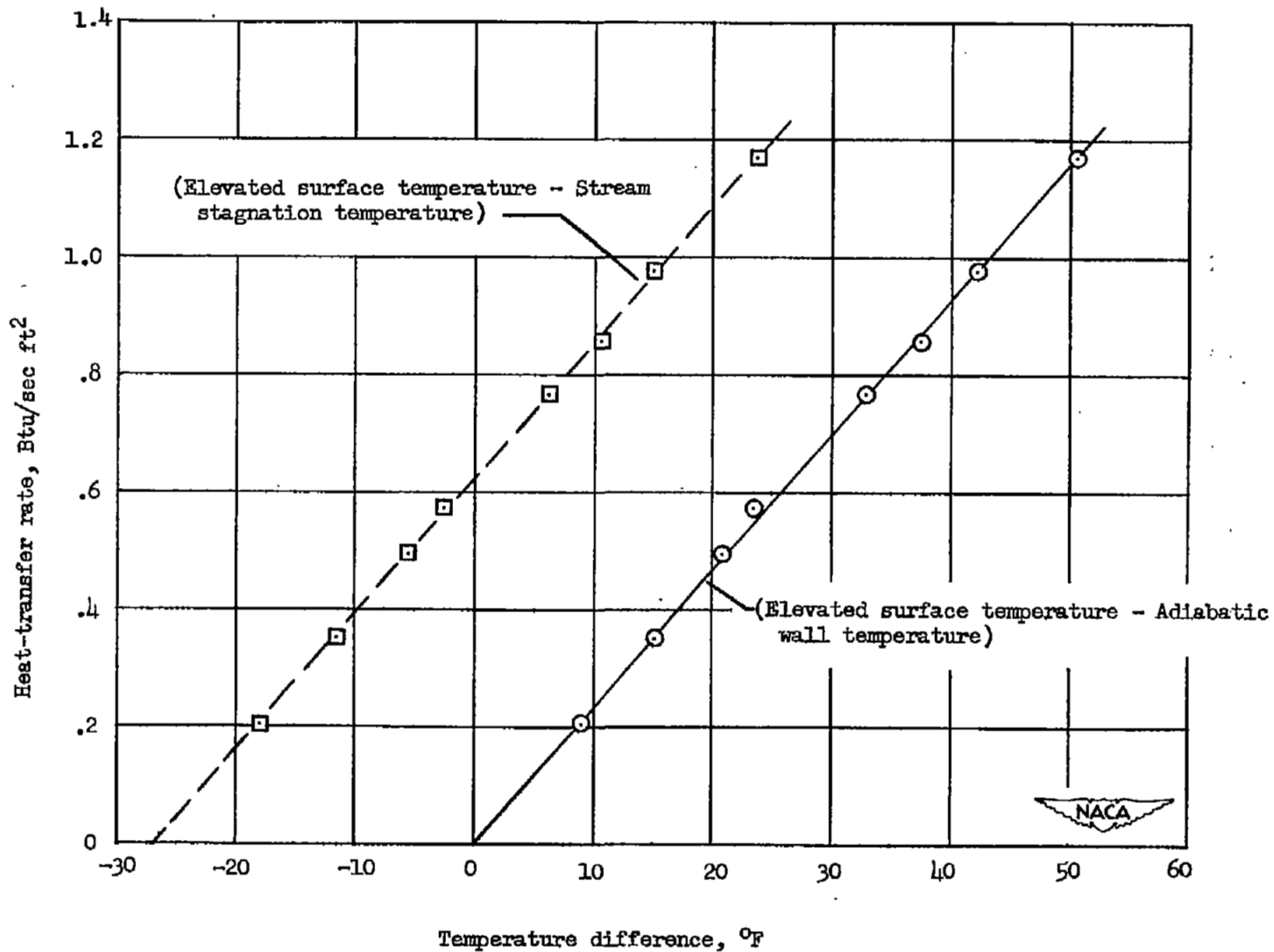


Figure 7.- Variation of heat-transfer rate with temperature difference.

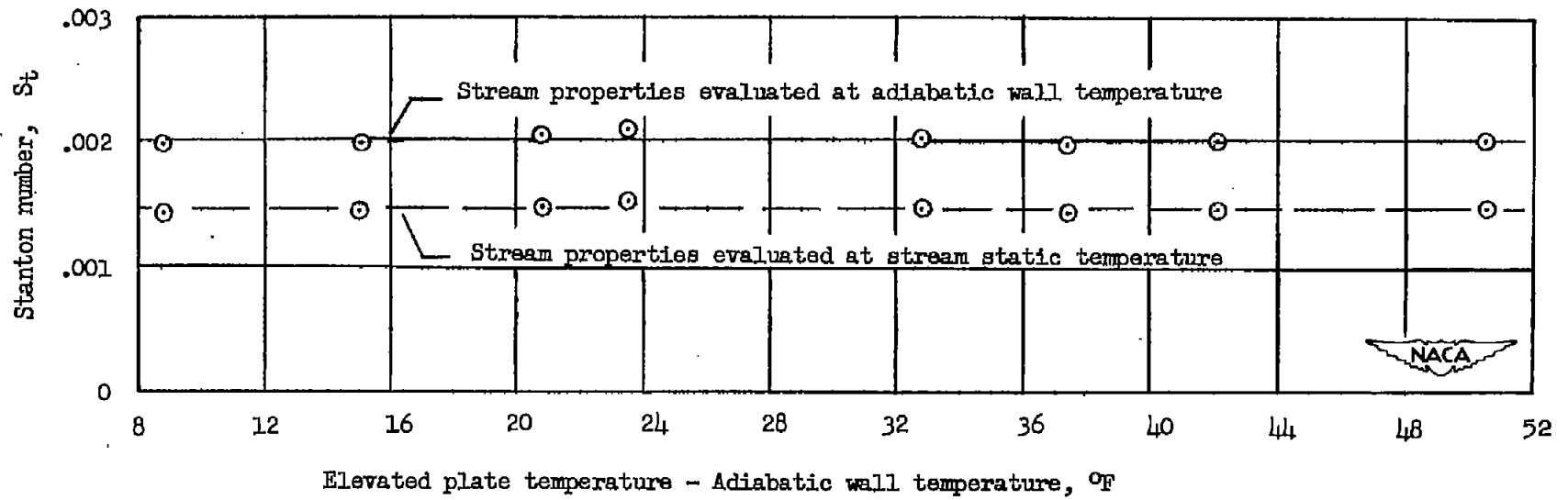


Figure 8.- Variation of Stanton number with temperature potential.

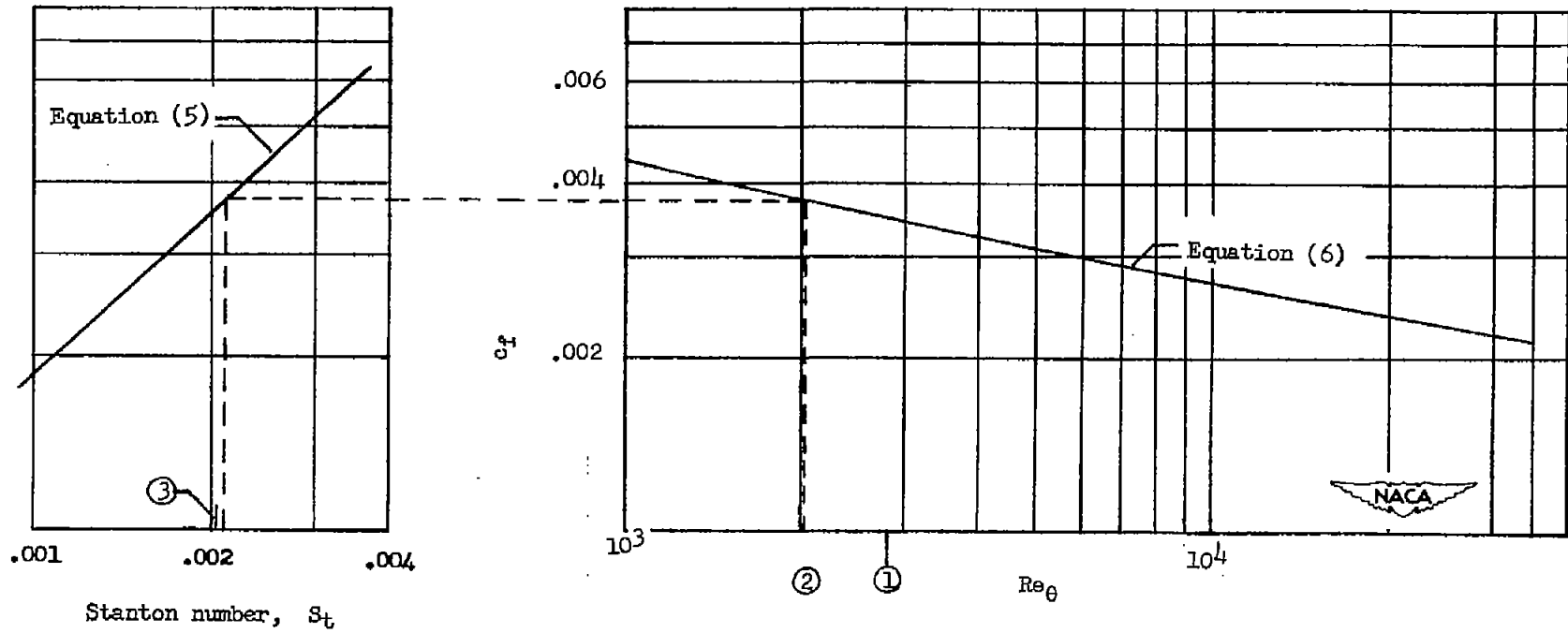


Figure 9.- Variation of skin-friction coefficient with Stanton and Reynolds numbers. Stream properties evaluated at adiabatic wall temperature.

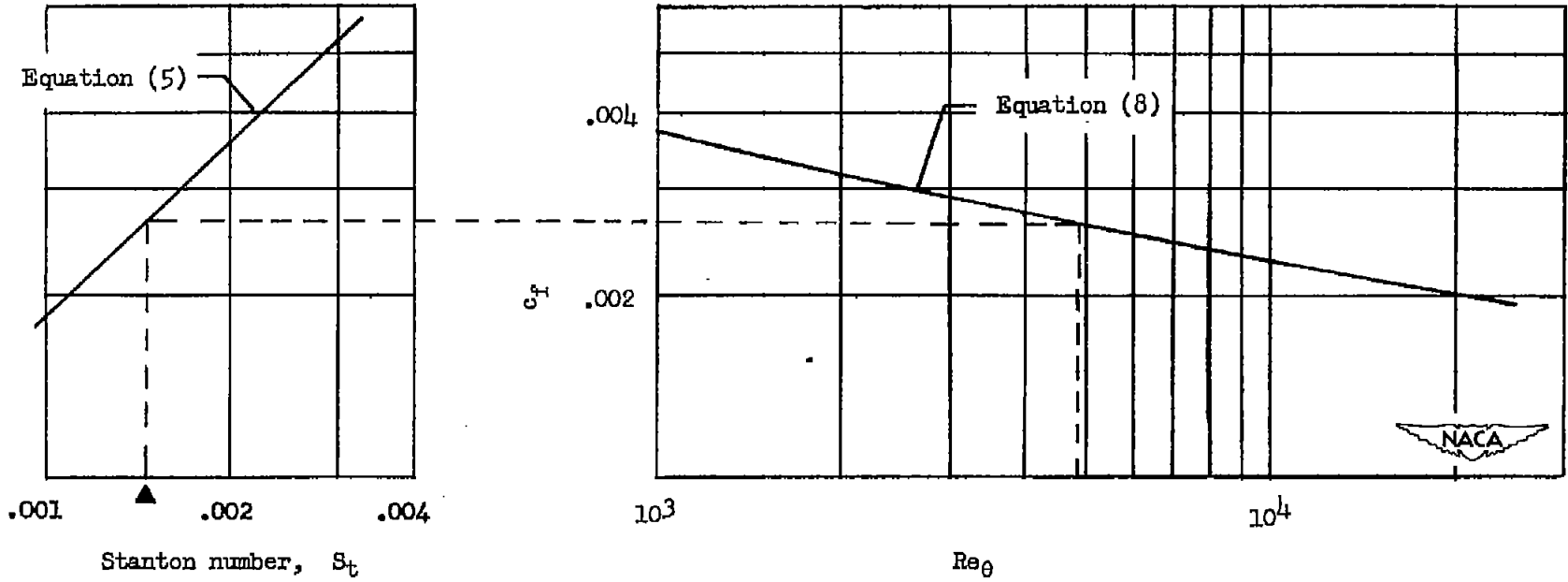


Figure 10.- Variation of skin-friction coefficient with Stanton and Reynolds numbers. Stream properties evaluated at stream static temperature.

SECUR

INFORMATION

NASA Technical Library



3 1176 01436 4526

